Mining Science and Technology (China) 21 (2011) 273–276

Contents lists available at ScienceDirect

Mining Science and Technology (China)

journal homepage: www.elsevier.com/locate/mstc

Modeling of titration experiments by a reactive transport model

Ma Hongyun [a,*], Samper Javier [b], Xin Xin [c]

[a] *Xi'an Center of Geological Survey, Xi'an 710054, China*
[b] *Civil Engineering School, University of A Coruña, A Coruña 15008, Spain*
[c] *School of Environment and Resources, Jilin University, Changchun 130026, China*

ARTICLE INFO

Article history:
Received 27 September 2010
Received in revised form
30 October 2010
Accepted 20 November 2010

Keywords:
Titration experiment
Reactive transport model
Buffering mechanism
Base neutralization capacity

ABSTRACT

Acid mine drainage (AMD) is commonly treated by neutralization with alkaline substances. This treatment is supported by titration experiments that illustrate the buffering mechanisms and estimate the base neutralization capacity (BNC) of the AMD. Detailed explanation of titration curves requires modeling with a hydro-chemical model. In this study the titration curves of water samples from the drainage of the As Pontes mine and the corresponding dumps have been investigated and six buffers are selected by analyzing those curves. Titration curves have been simulated by a reactive transport model to discover the detailed buffering mechanisms. These simulations show seven regions involving different buffering mechanism. The BNC is primarily from buffers of dissolved Fe, Al and hydrogen sulfate. The BNC can be approximated by: $BNC = 3(C_{Fe} + C_{Al}) + 0.05C_{sulfate}$, where the units are mol/L. The BNC of the sample from the mine is 9.25×10^{-3} mol/L and that of the dumps sample is 1.28×10^{-2} mol/L.

1. Introduction

Mine activities may pose severe impacts in water resources and ecosystems when pyrite-rich materials from those activities are exposed to atmospheric conditions and then generate acid mine drainage (AMD) waters. AMD is characterized by high acidity (pH 2–4), high sulfate concentrations (1–20 g/L) and large concentrations of metals such as Fe, Mn, or Al [2–10,15]. Isolating mine wastes from the atmosphere is expected to decrease AMD generation. Neutralizing AMD with alkaline substances is a common and effective treatment for AMD water [1,5–8].

Titration is used to investigate the Base Neutralization Capacity (BNC) of discharged water. Buffering systems in the AMD sample can be described by titration curves that relate pH to acidity. A detailed understanding of the buffering mechanisms relevant to acid mine drainage neutralization can be obtained by hydro-chemical modeling [12,13].

In this study, the titration curves of acidic waters from the As Pontes mine lake, and the dumps located in Galicia (N.W. Spain) were investigated and reproduced by geochemical modeling. The objective was to obtain a detailed understanding and quantitative description of buffering mechanisms relevant to AMD waters neutralization.

2. Materials and methods

The study was performed on water from the As Pontes Coal Mine in Galicia north-west Spain. Mining ended there in December, 2007. Mining left a big open pit with a volume of 547 hm^3 and a tailings dump with a surface area of 11.4 km^2. AMD water is generated in the mine pit and the dumps areas even though land treatment was performed properly [11]. Samples from the mine and the dumps were titrated with 0.1 N NaOH at a rate of 0.5 mL/min. The initial volume of each sample was 100 mL. The chemical composition of drainage water samples from the mine and the tailing dumps is shown in Table 1.

The titration curves were simulated using a multi-component reactive transport code, CORE^{2D}V4 (Javier Samper, 2003), to characterize the buffering mechanisms and to describe contributions from each acid–base pair to the BNC.

The geochemical model considers the following chemical reactions: aqueous complexation, acid–base, redox, mineral dissolution/precipitation, gas solution/exsolution and surface complexation. The chemical system is defined in terms of the following 14 primary species, H_2O, H^+, Ca^{2+}, Mg^{2+}, Na^+, K^+, Fe, Mn, Al, Cl^-, $SO_4{}^{2-}$, $HCO_3{}^-$, $SiO_{2(aq)}$, $O_{2(aq)}$, and a surface complex, XOH. Relevant aqueous complexes were identified from speciation runs performed with EQ3/6 (Wolery, 1992).

3. Titration curve analysis

Buffering in a titration curve shows up as a buffering plane where the slope of the curve decreases. Titration curves of the two

---

[*] Corresponding author. Tel.: +86 29 87821984.
E-mail address: mhy19809730@126.com (M. Hongyun).

1674-5264/$ – see front matter Copyright © 2011, China University of Mining & Technology. All rights reserved.
doi:10.1016/j.mstc.2011.02.006

Table 1
Composition of drainage water samples from the mine and the tailing dumps (mol/L).

	Mine pit	Dumps
pH	2.9	2.8
Na^+	1.21×10^{-3}	8.69×10^{-4}
K^+	7.67×10^{-5}	1.91×10^{-4}
Mg^{2+}	2.46×10^{-3}	1.02×10^{-2}
Ca^{2+}	5.00×10^{-3}	1.00×10^{-2}
Fe total	1.48×10^{-3}	2.81×10^{-3}
Al total	1.02×10^{-3}	4.02×10^{-4}
Mn total	2.51×10^{-3}	1.18×10^{-3}
SO_4^{2-}	3.49×10^{-2}	6.51×10^{-2}
Cl^-	2.11×10^{-4}	7.33×10^{-4}
HCO_3^-	1.64×10^{-8}	1.66×10^{-8}
$SiO_{2(aq)}$	3.90×10^{-4}	3.90×10^{-4}

Table 2
Surface complexation reactions [14].

Surface complex	log K_{int}
$\equiv XOH_2^+ \Leftrightarrow \equiv XOH + H^+$	−7.29
$\equiv XO^- \Leftrightarrow \equiv XOH - H^+$	8.93
$\equiv XSO_4^- \Leftrightarrow \equiv XOH + SO_4^{2-} + H^+ - H_2O$	−7.78
$\equiv XOHSO_4^{2-} \Leftrightarrow \equiv XOH + SO_4^{2-}$	−0.79
$\equiv XOCa^+ \Leftrightarrow \equiv XOH + Ca^{2+} - H^+$	5.15
$\equiv XOMg^+ \Leftrightarrow \equiv XOH + Mg^{2+} - H^+$	4.60

types of samples are presented in Figs. 1 and 2. Fig. 1 shows that there are three apparent buffering planes in the titration curve of mine pit samples. Plane I indicates iron buffering and Plane II indicates aluminum buffering, according to the literature [14]. Buffering Plane III (pH ≈ 9.5) has not been found in any published literature. However, the simulation shows that if an initial $O_{2(aq)}$ concentration about 10^{-33} mol/L is adopted manganese precipitation could then explain this buffering. The titration curve of the dumps, Fig. 2, also shows three apparent buffering planes. It is apparent that Plane IV is caused by the same buffering mechanism as Plane I, and that Planes VI and III have the same origin, but Planes V and II indicate different buffers. The Al buffering plane did not appear because of the low concentration of dissolved Al in the dumps sample (see Table 1). Plane V is caused by the transformation of Fe from schwertmannite to $Fe(OH)_{3(s)}$. This buffering plane does not appear in Fig. 1 because the mine pit water has a smaller concentration of dissolved Fe.

According to this analysis it is assumed that there are at least five different buffering mechanisms present in the discharge water.

1) The slow increase before Plane I (pH < 3.0) is controlled by free hydrogen and hydrogen sulfate buffering. In this stage, titrated alkalis are neutralized until most HSO_4^- and protons are consumed:

$$H^+ = H_2O - OH^- \qquad \log K = 14.00$$

$$HSO_4^- = SO_4^{2-} + H^+ \qquad \log K = -1.978$$

2) Buffering Plane IV (pH ≈ 3.0) indicates iron buffering. The dissolution/precipitation of iron minerals ($Fe(OH)_{3(s)}$ and schwertmannite) provides this buffering. The reactions are:

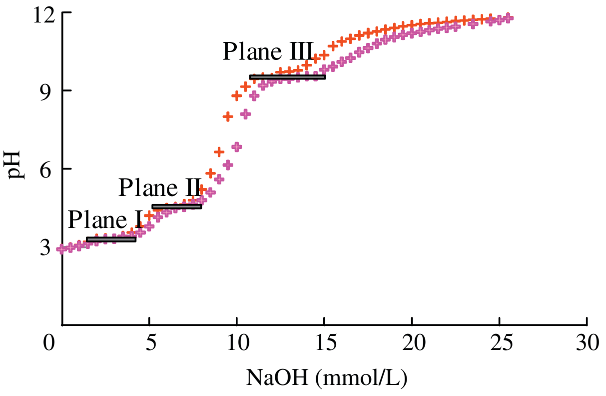

Fig. 1. Measured titration curve of AMD water from the mine at As Pontes.

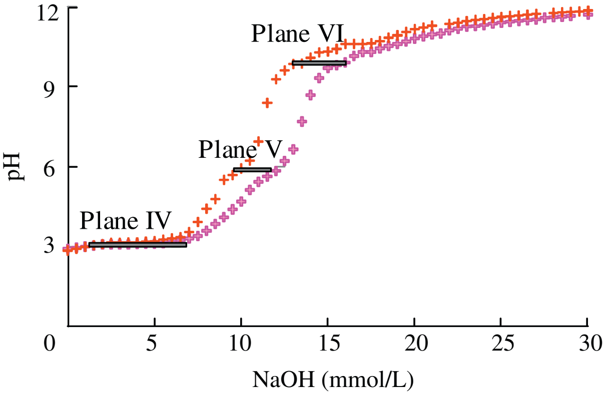

Fig. 2. Measured titration curve of AMD water from the dumps at As Pontes.

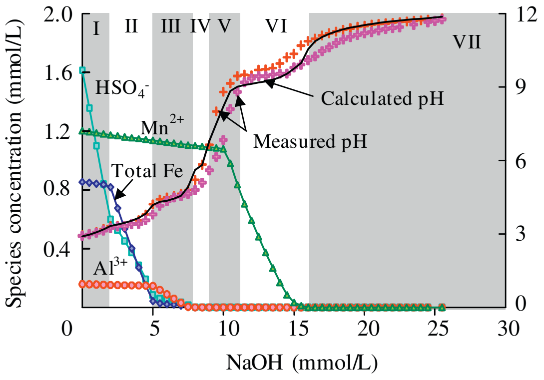

Fig. 3. Measured and calculated titration curves and concentrations of aqueous species: mine sample (gray bands show the different buffering regions).

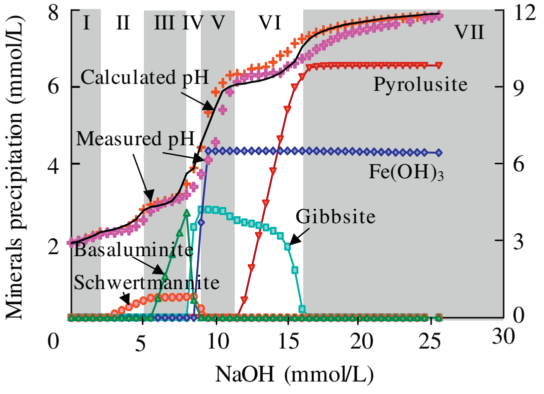

Fig. 4. Measured and calculated titration curves and cumulative mineral dissolution/precipitation: mine sample.

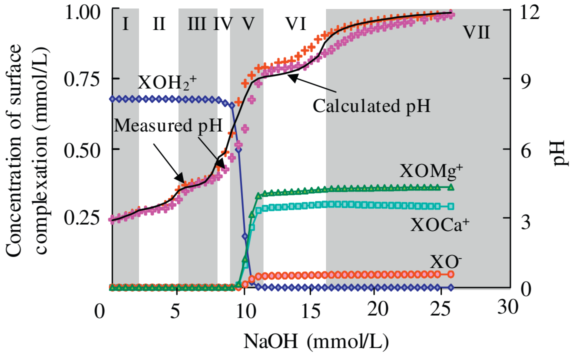

Fig. 5. Measured and calculated titration curves and concentrations of the surface complexes: mine sample.

$Fe(OH)_{3(s)} = Fe^{3+} + 3H_2O - 3H^+ \quad \log K = 4.90$

$Fe_8O_4(OH)_{12}(SO_4)_{2(s)} = 8Fe^{3+} + 2SO_4{}^{2-} + 16H_2O - 20H^+$
$\log K = 12.00$

3) Buffering Plane II ($pH \approx 4.5$) indicates aluminum buffering. This buffer is associated with the dissolution/precipitation of aluminum minerals (gibbsite and basaluminite). The main reactions are:

$Al(OH)_3 = Al^{3+} + 3H_2O - 3H^+ \quad \log K = 9.00$

$Al(SO_4)_{0.25}(OH)_{2.5} = Al^{3+} + 0.25SO_4{}^{2-} + 2.5H_2O - 2.5H^+$
$\log K = 5.70$

4) The slow increase between Planes V and VI ($6.0 < pH < 9.5$) indicates surface complexation buffering [14]. Surface complexation reactions are known to occur at the surface of minerals. A fixed site model is used to model this surface complexation buffering. The reactions are listed in Table 2. The sorption site concentrations are set to 20% of the concentration of the main minerals, 8.10×10^{-4} mol/L for the mine sample and 1.55×10^{-3} mol/L for the sample from the dumps.
5) Buffering Planes III and VI ($pH \approx 9.6$) indicate manganese buffering. Pyrolusite precipitation/dissolution was included in the geochemical modeling though this reaction:

$MnO_{2(s)} = Mn^{2+} + 0.5O_{2(aq)} + H_2O - 2H^+ \quad \log K = -1.44$

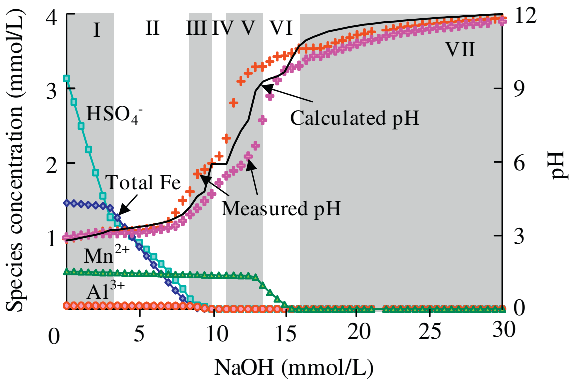

Fig. 6. Measured and calculated titration curves and concentrations of aqueous species: dumps sample.

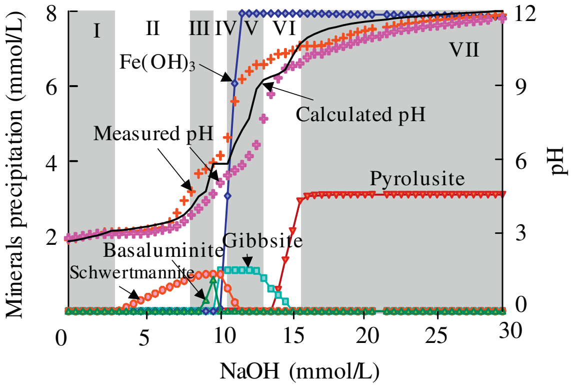

Fig. 7. Measured and calculated titration curves and cumulative mineral dissolution/precipitation: dumps sample.

4. Results and discussion

The titration curves were reproduced by the geochemical model after adjusting the setting of the different buffering systems. Then the titration curves were compared to the evolution of aqueous specie concentrations (see Figs. 3 and 6), cumulative mineral precipitation/dissolution (see Figs. 4 and 7) and surface complexes (see Figs. 5 and 8) to analyse the structure of the buffering systems and to quantify the capacity of each buffering mechanism. This shows that the titration curves can be divided into seven sections having the following buffering mechanisms.

1) Free hydrogen ions and hydrogen sulfate ($pH < 3.0$): In this stage, hydrogen sulfate is the main base and $HSO_4{}^-$ decreases quickly while pH increases slowly.
2) Schwertmannite precipitation ($3.0 < pH < 3.4$): Fe precipitates as schwertmannite in this stage.
3) Basaluminite precipitation ($3.4 < pH < 6.0$)
4) Transformation of schwertmannite to $Fe(OH)_{3(s)}$ and of the aluminum mineral basaluminite to gibbsite ($pH \approx 6.0$)
5) Surface complexation ($6.0 < pH < 9.0$). In this stage, surface complexes transform from $XOH_2{}^+$ to $XOCa^+$, $XOMg^+$, or XO^- as the pH increases from 6.0 to 9.0.
6) Mn precipitation and aqueous complexation of $Al(OH)_4{}^-$ ($9.0 < pH < 10.8$): Pyrolusite precipitation is controlled by the redox conditions of the water sample. It is assumed that this buffering stage is caused by Mn precipitation and the dissolution of gibbsite.
7) Aqueous complexes such as $Fe(OH)_4{}^-$ ($pH > 10.8$).

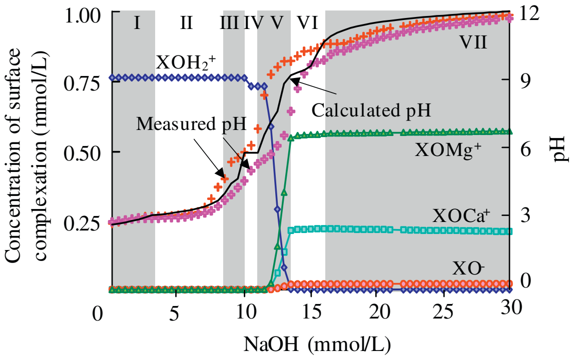

Fig. 8. Measured and calculated titration curves and concentrations of the surface complexes: dumps sample.

The Base Neutralization Capacity (BNC) includes mainly three acid buffers: hydrogen sulfate HSO_4^-, which is about 5% of the total sulfate according to the speciation estimates determined using EQ3/6, dissolved Fe, and dissolved Al. The BNC value can be approximated from:

$$\mathrm{BNC\ (mol/L)} = 3(C_{\mathrm{Fe}} + C_{\mathrm{Al}}) + 1/20 \cdot C_{\mathrm{sulfate}}$$

where C indicates the dissolved concentration.

The BNC of the sample from the mine is 9.25×10^{-3} mol/L and that of the dumps sample is 1.28×10^{-2} mol/L.

5. Conclusions

Titration experiments are basic measurements for determining waste water acidity. Geochemical modeling can help analyse the acid–base buffering reactions and to quantify the neutralization capacity. In this study, one from the As Pontes Coal Mine pit and the other from the corresponding dumps were investigated. Titration curves were analysed and modeled using a reactive transport model, CORE^{2D}V4. The main conclusions are:

1) Titration curves of both samples are similar, and they show the same kind of buffering mechanisms. This indicates that acid mine drainage from the mine and the dumps had similar environmental conditions when it was formed.
2) Five buffering species-free hydrogen, hydrogen sulfate, and dissolved Fe, Al and Mn and surface complexation are required to construct the buffering systems.
3) The base neutralization capacity (BNC) is primarily controlled by buffer reactions involving Fe, Al, and hydrogen sulfate. BNC can be approximated by: $\mathrm{BNC} = 3(C_{\mathrm{Fe}} + C_{\mathrm{Al}}) + 0.05C_{\mathrm{sulfate}}$.

References

[1] Amos RT, Mayer KU, Blowes DW, Ptacek CJ. Reactive transport modeling of column experiments for the remediation of acid mine drainage. Environmental Science and Technology 2004;38:3131–8.

[2] Appelo CAJ, Postma D. Geochemistry, groundwater and pollution. Rotterdam: Balkema; 1993.

[3] Bian ZF, Inyang HI, Daniels JL, Otto F, Struthers S. Environmental issues from coal mining and their solutions. Mining Science and Technology 2010;20:215–23.

[4] Bigham JM, Nordstrom DK. Iron and aluminum hydroxysulfates from acid sulfate waters. In: Alpers CN, Jambor JL, Nordstrom DK, editors. Sulfate minerals: crystallography, geochemistry and environmental significance. Reviews in Mineralogy and Geochemistry, vol. 40; 2000. p. 351–403.

[5] Christopher GH, Stuart B, Max LC. Aqueous geochemistry and oxygen isotope compositions of acid mine drainage from the Río Tinto, SW Spain, highlight inconsistencies in current models. Chemical Geology 2009;265:321–34.

[6] Diz HR. Chemical and biological treatment of acid mine drainage for the removal of heavy metals and acidity. Virginia Polytechnic Institute and State University; 1997.

[7] Gitari WM, Petrik LF, Etchebers O, Key DL, Iwuoha E, Okujeni C. Treatment of acid mine drainage with fly ash: removal of major contaminants and trace elements. Journal of Environmental Science and Health Part A 2006;A41:1729–47.

[8] Gitari WM, Petrik LF, Etchebers O, Key DL, Iwuoha E, Okujeni C. Passive neutralization of acid mine drainage by fly ash and its derivatives: a column leaching study. Fuel 2008;87:1637–50.

[9] Gu GH, Su LJ, Chen ML, Sun XJ, Zhou HB. Bio-leaching effects of Leptospirillum ferriphilum on the surface chemical properties of pyrite. Mining Science and Technology 2010;20:286–91.

[10] He XW, Yang HM, He Y. Treatment of mine water high in Fe and Mn by modified manganese sand. Mining Science and Technology 2010;20:571–5.

[11] Ma HY. Multicomponent reactive transport models for acid mine drainage and radioactive waste disposal. A Coruña, Spain: University of A Coruña; 2010.

[12] Oliver T, Andrew F, Margarete K. Titration curves: a useful instrument for assessing the buffer systems of acidic mining waters. Environmental Science and Pollution Research 2006;13:215–24.

[13] Shan Y, Qin Y, Wang WF. Chromium leaching mechanism of coal mine water-a modeling study based on Xuzhou-Datun coal mine district. Mining Science and Technology 2010;20:97–102.

[14] Uhlmann W, Buttcher H, Totsche O, Steinberg CEW. Buffering of acidic mine lakes: the relevance of surface exchange and solidbound sulphate. Mine Water and Environment 2004;23:20–7.

[15] Younger PL, Banwart SA, Hedin RS. Mine water: hydrology, pollution, remediation. Dordrecht: Kluwer Academic Publishers; 2002.